JACS
JOURNAL OF THE AMERICAN CHEMICAL SOCIETY
Communication
Cite This: J. Am. Chem. Soc. 2019, 141, 1425−1429
pubs.acs.org/JACS

Deciphering Determinants in Ribosomal Methyltransferases That Confer Antimicrobial Resistance

Ruchika Bhujbalrao and Ruchi Anand*

Department of Chemistry, Indian Institute of Technology Bombay, Powai, Mumbai 400076, India

Supporting Information

ABSTRACT: Post-translational methylation of rRNA at select positions is a prevalent resistance mechanism adopted by pathogens. In this work, KsgA, a housekeeping ribosomal methyltransferase (rMtase) involved in ribosome biogenesis, was exploited as a model system to delineate the specific targeting determinants that impart substrate specificity to rMtases. With a combination of evolutionary and structure-guided approaches, a set of chimeras were created that altered the targeting specificity of KsgA such that it acted similarly to erythromycin-resistant methyltransferases (Erms), rMtases found in multidrug-resistant pathogens. The results revealed that specific loop embellishments on the basic Rossmann fold are key determinants in the selection of the cognate RNA. Moreover, in vivo studies confirmed that chimeric constructs are competent in imparting macrolide resistance. This work explores the factors that govern the emergence of resistance and paves the way for the design of specific inhibitors useful in reversing antibiotic resistance.

The growing resistance of pathogens to antibiotics is a silent epidemic projected to kill more than 300 million people by 2050.[1] The situation has worsened, as superbugs such as MRSA, NDM-1, CRE, XR-Mtb, and others have now become resistant to the last line of next-generation semisynthetic derivatives such as azithromycin and clarithromycin.[2] Therefore, there is a pressing need to delve deeper into the origins of resistance and find ways to resensitize pathogens to existing antibiotics.[3] Bacterial adaptation to antibiotics highlights the immense genetic plasticity of these organisms and is a pinnacle of evolution. Pathogens commonly gain resistance either through mutational adaptation or via transfer of specific genetic elements via lateral gene transfer.[4] For instance, resistance against the very successful β-lactam class of drugs was developed through the acquisition of antibiotic degraders such as β-lactamases.[5] Another common mechanism through which resistance is gained through the covalent modification of ribosomes, which are targeted by several antibiotics.[6] Macrolides such as erythromycin, along with lincosamide and streptogramins, operate by acting as molecular blocks and inhibit protein translation by binding to the protein exit tunnel within the ribosomes.[6,7] Enzymes such as Erms induce resistance by post-translationally modifying the exocyclic N6 of A2058 rRNA (*Escherichia coli* numbering).[6,7] Methylation at A2058 (G in humans) causes a steric clash and displaces the antibiotic from the ribosomes.[8] Most pathogens have both mono- and dimethyltransferases: the single epigenetic methyl mark confers moderate levels of resistance, whereas dimethylation results in an aggressive resistance phenotype (Scheme 1).[9]

Scheme 1. Representative Methylation Reactions

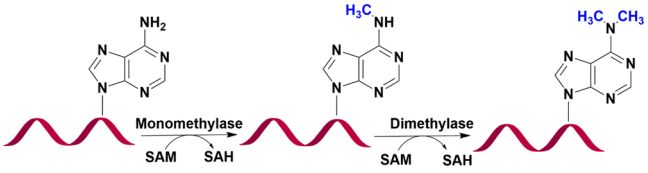

Methylation by Erms occurs via the universal methyl donor *S*-adenosylmethionine (SAM).[10] SAM-dependent methylation is a ubiquitous modification that not only occurs in RNA but is also an epigenetic mark conferred on both DNA and proteins that govern gene regulation.[11] For instance, lysine methylation in histones suppresses gene expression by condensing chromatin, whereas DNA methylation has a similar effect via the formation of CpG islands.[12,13] Structurally, most SAM-dependent methyltransferases adopt a canonical Rossman fold in which the central active site catalyzes methyl transfer via an S_N2-mediated transition state.[14,15] Despite the structural and mechanistic similarity among these diverse methyltransferases (Mtases), the enzymes are specific toward their respective substrates. The targeting mechanism is fine-tuned to such a degree that even among rMtases, two different enzymes catalyze only at the desired specific ribosomal position.[16] However, the determinants controlling this high level of catalytic finesse remain elusive.

To address this issue, we explored the structural mechanism responsible for targeting. As a model system, we chose a housekeeping rMtase, KsgA, present in all bacteria that catalyze dimethylation at adjacent adenosine bases A1518 and A1519 of 16S rRNA.[17,18] The X-ray structures of apo- and SAM bound forms of *Bacillus subtilis* KsgA (BsKsgA) were solved to 1.9 Å. Structural and phylogenetic analysis were used as guides to generate KsgA chimeras with switched targeting propensities. These studies aided in unearthing determinants that help convert a nonpathogenic rMtase, KsgA, to a pathogenic Erm. These findings help understand how nature alters specificity while maintaining a conserved catalytic mechanism. Moreover,

Received: October 2, 2018
Published: January 9, 2019

DOI: 10.1021/jacs.8b10277
J. Am. Chem. Soc. 2019, 141, 1425−1429

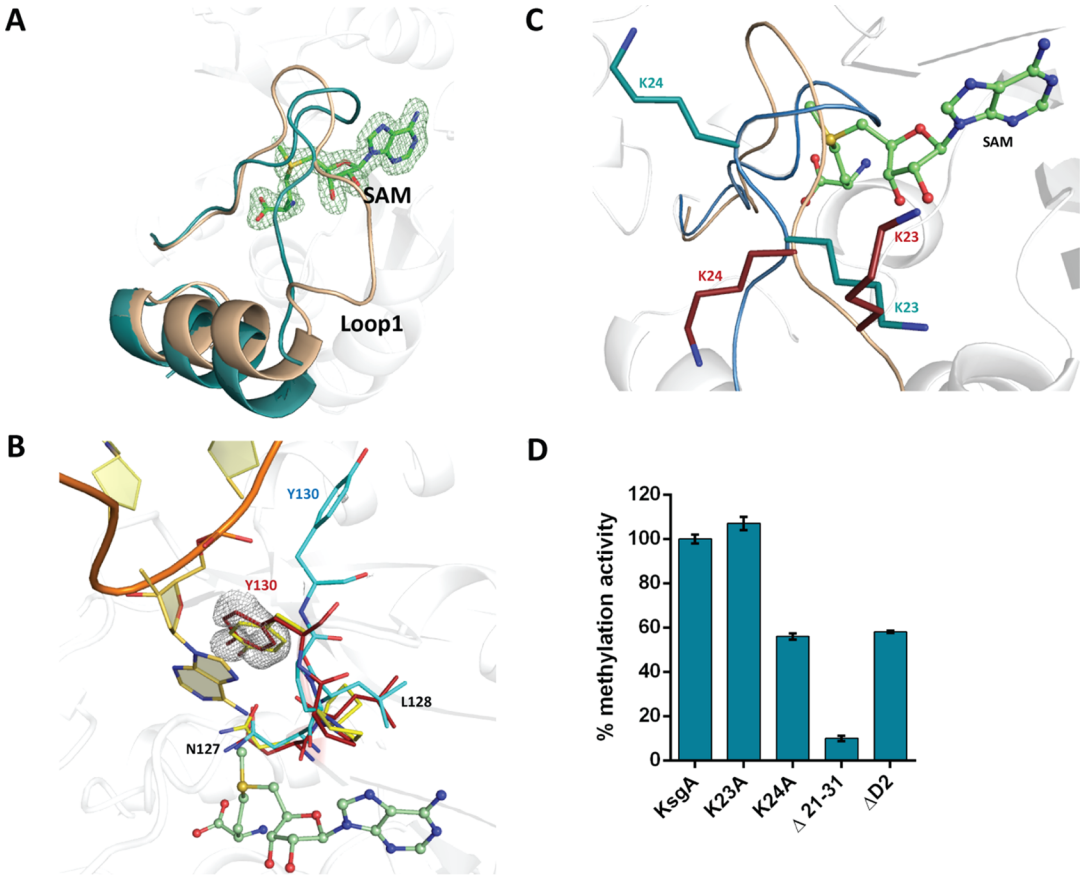

Figure 1. Role played by the N-terminal loop. (A) Conformational changes in BsKsgA upon SAM binding (brown, PDB: 6IFS; cyan, PDB: 6IFT). The Fo−Fc density (green) is countered at 3σ. (B) Rearrangement of Y130 upon SAM binding (red) shows correspondence with a catalytically competent conformation observed in DNA Mtase (yellow, PDB: 1G38). (C) Zoom view of loop1 highlighting the motion of positively charged residues. In all structures, oxygen and nitrogen atoms appear in red and blue, respectively. (D) In vitro assay with ^{3}H-methyl-SAM using 30S ribosomal subunit as the substrate.

this knowledge serves as a path toward the development of inhibitors that target the RNA recognition region rather than the common SAM binding region.

Similar to other rMtases, BsKsgA consists of two domains: an N-terminal catalytic domain harboring the Rossmann fold, and a small C-terminal head domain (Figure S1A). Multiple structures of KsgA from organisms such as *E. coli* and thermophilic species have previously been determined.[17,19] However, these structures were unable to completely capture the active site environment, as either the loop adjacent to the SAM binding site was disordered or the aminopropyl group of SAM could not be visualized.[19,20] In the BsKsgA structure, we were able to observe clear density for SAM in its entirety (Figure 1A, S1B). The structural investigation revealed that the ordering of the propyl group primes KsgA for interaction with the RNA. For instance, Y130 in the SAM bound structure adopts an inward conformation similar to that observed in DNA methyltransferases (Figure 1B).[21] Superposition of the SAM bound structures of BsKsgA and ErmC′ shows that loop1 is significantly divergent in both enzymes, in sequence as well as in length (Figure S1C). While loop1 was found to be disordered even upon SAM binding in Erms, a major structural rearrangement (rmsd of 4.2 Å) in this region was observed in BsKsgA. Positively charged lysine residues K23 and K24 rearrange, which results in the simultaneous closure of the conserved QNF motif onto the aminopropyl group of SAM, thereby aiding in stabilization (Figure 1C, S2A). Based on the above information, it was proposed that loop1 serves as an entry platform for rRNA binding.

To test this hypothesis, we cloned, expressed, and purified K23A, K24A and deletion mutant Δ21−31. Further, the methyl donation efficiency was monitored via the transfer of the tritium label of 3H-methyl-SAM to the cognate 30S ribosome (Supporting Information methods). As expected, deletion of the central flexible loop1 region resulted in complete obliteration of activity, as Δ21−31 construct could not bind to SAM (Figure S2B). Although K23A mutation has no effect on activity, removal of the seemingly surface-exposed lysine K24A yields in reduction of activity by 50% (Figure 1D). This significant loss of activity due to K24A mutation remained perplexing. To understand this observation, we superimposed the SAM bound BsKsgA structure on the 13 Å cryo-EM *E. coli* ribosome−KsgA complex.[22] This comparison revealed that K24A plays a critical role in anchoring the protein to rRNA via interaction with the phosphate backbone (Figure S2C). Given all the above factors, loop1 was selected as a target site for tweaking the rRNA propensity of KsgA.

Comparison of additional features of both enzymes revealed that KsgA is more stringent and accepts only a 30S ribosomal subunit as a substrate, whereas ErmC′ can catalyze mini-RNA substrates that mimic the local ribosomal environment.[10,23,24] Other notable differences between the ErmC′ and KsgA substrates are in the topology and local structure of the RNA both the proteins catalyze (Figure 2A,B,C).[25] Therefore,

DOI: 10.1021/jacs.8b10277
J. Am. Chem. Soc. 2019, 141, 1425−1429

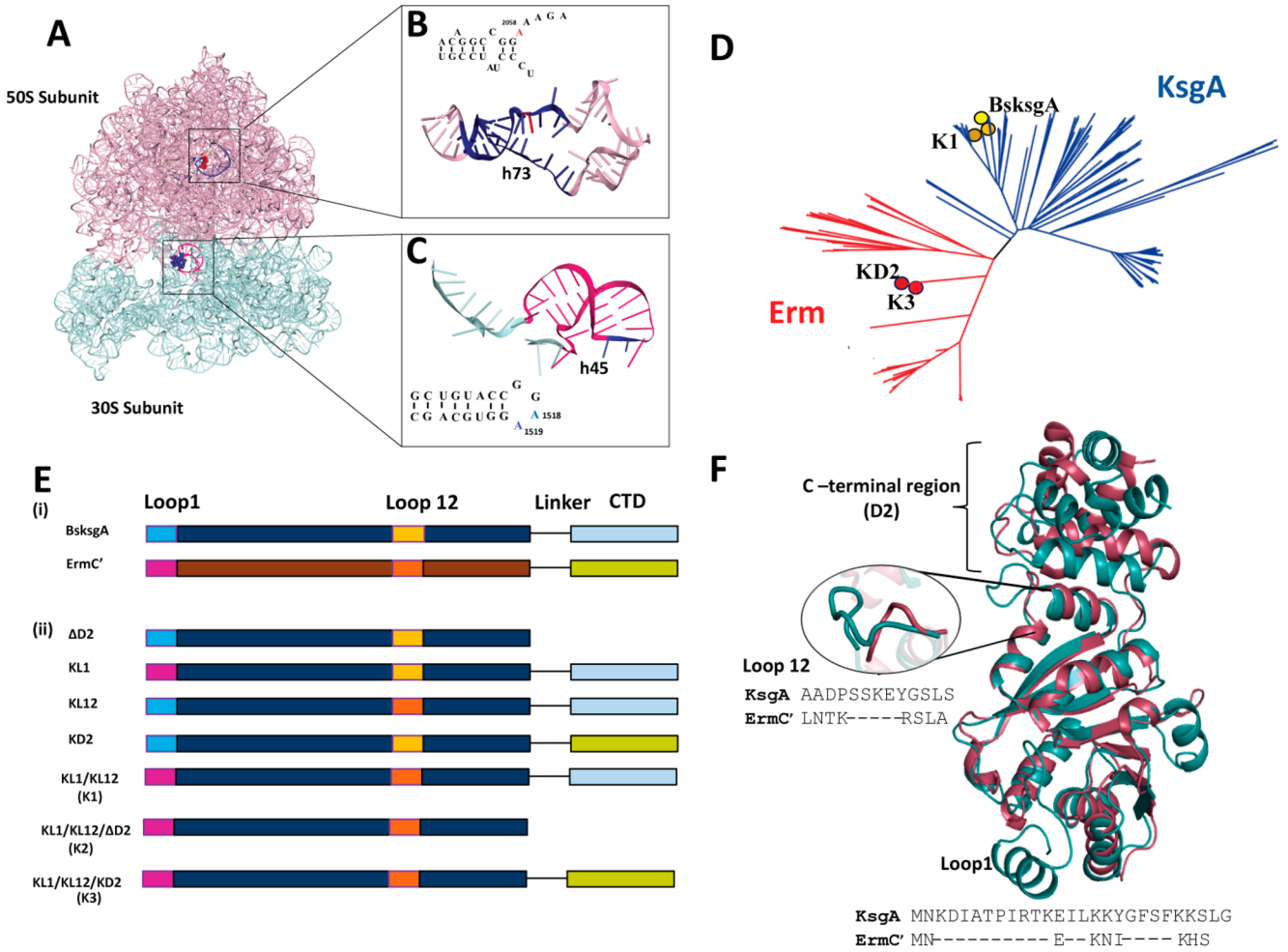

Figure 2. Design of chimeras to switch targeting propensity. (A) Overall architecture of bacterial 70S ribosome (PDB ID: 3J3V), ribosomal subunits, and 50S (pink) and 30S (blue) subunits. (B and C) Close-up view of Mtase targets sites. (D) Phylogenetic tree constructed using the maximum likelihood method. Chimeras K3 and KD2 are evolutionarily close to Erms. (E) Naming and design of native and chimeras. (F) Structural alignment of BsKsgA (teal) and ErmC′ (pink; PDB ID: 1QAM) used as a guide for creation of the chimeras. Structural and sequence differences are highlighted in the inset.

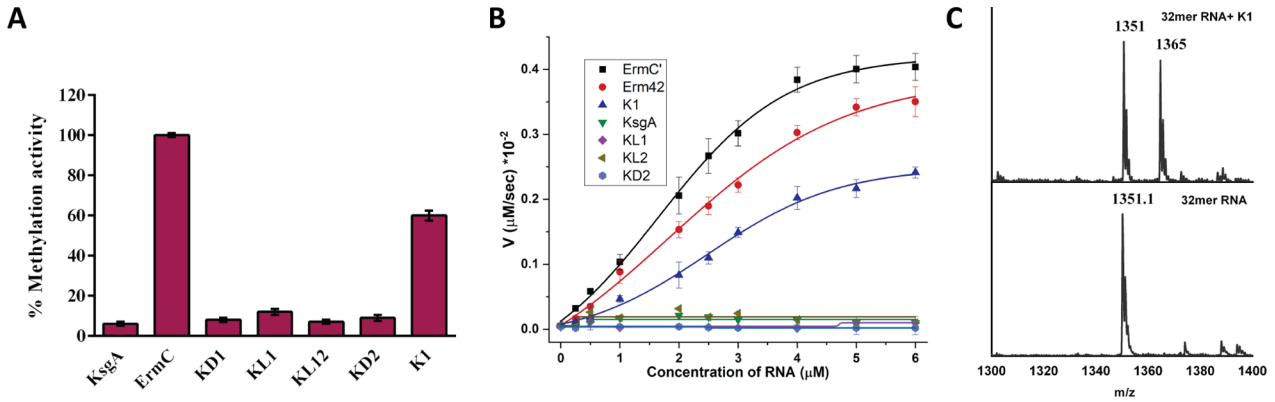

Figure 3. Activity assay of chimeras toward the Erm mini-RNA substrate. (A) Scintillation assay. (B) Steady-state kinetics with the mini-RNA Erm substrate. The chimera K1, in which both the loops were replaced, showed 50% methylation efficiency. (C) MALDI-TOF for chimera K1. A shift in molecular mass by 14 Da is indicative of methylation.

phylogenetic and the structural examinations were employed to find structural elements in the two proteins that can differentiate the unique RNA structures. The above analysis showed that another element namely, loop12 may play a critical role in determining target propensities (Figure 2D,F). Apart from adopting a different conformation in the two proteins, loop12 interfaces between the central SAM binding domain and is also consistently shorter in ErmC′ by five amino acids. Docking of the ErmC′ RNA site revealed that in Erms, loop12 stabilizes the RNA (Figure S4A). On the contrary, in

DOI: 10.1021/jacs.8b10277
J. Am. Chem. Soc. 2019, 141, 1425−1429

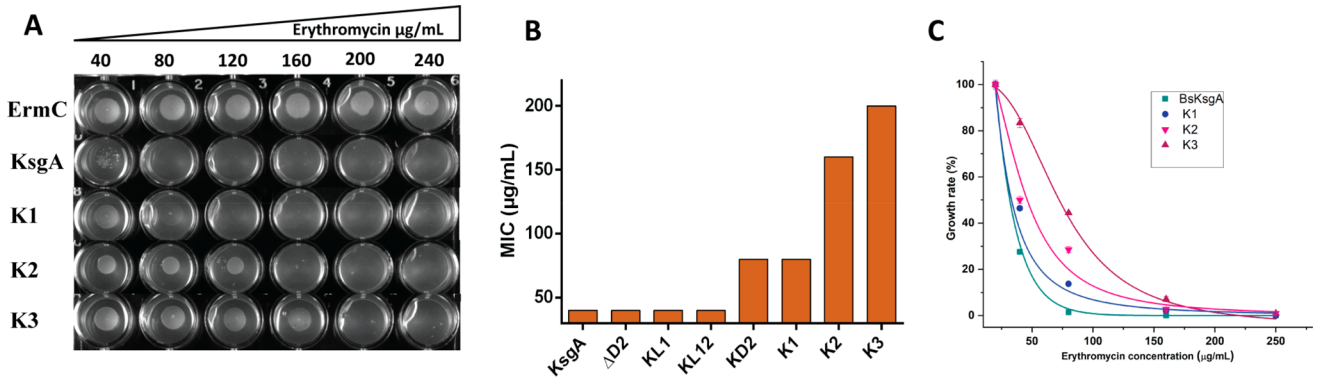

Figure 4. Sensitivity of chimeras toward the macrolide antibiotic erythromycin in vivo. (A) Spot assay for chimeras with increasing erythromycin concentration. (B) MIC studies with various chimeras. (C) Growth rate of chimeras in the presence of antibiotic.

KsgA, this loop clashes with the ErmC′ rRNA substrate, thereby preventing KsgA from accepting it (Figure S4B). Based on this analysis, loop12 along with loop1 was proposed to be responsible for substrate selectivity.

To confirm these predictions, we created a series of chimeric proteins in which loop1 or loop12 or both were exchanged onto a BsKsgA template (Figure 2E). Previous studies have shown that some tuberculosis strains have a variant, Erm37, that lacks the C-terminal head domain.[26] Erm37 displays promiscuous activity and methylates at adjacent positions in the vicinity of A2058.[26] Further, both ErmC′ and KsgA exhibit very low sequence conservation in the C-terminal head domain, and structural comparison reveals that rmsd in this domain is quite high (~5.5 Å). Therefore, we generated variants in which the head was deleted (ΔD2) and related chimeras that additionally had the loops switched (Figure 2E).

X-ray structures of KL1, KL12, and ΔD2 confirmed that the protein structure was not perturbed by these mutations (Figure S3, Table S1). Scintillation assays (transfer of tritium-labeled methyl group) showed that chimeras with the individual substitution of loops (chimeras KL1, KL12) do not exhibit methylation (Figure 3A). Chimera (KD2), in which the head domain of ErmC′ was stitched onto the BsKsgA scaffold, also showed no methylation. However, a chimera in which the dual loop1 and loop12 regions were switched exhibited significant methylation (Figure 3A, 3B) and had a catalytic efficiency that was 50% lower than that of the native Erm enzymes (ErmC′, Erm42; Table S2). These results were confirmed via MALDI-TOF assay (Figure 3C, Supporting Information methods). The results indicate that loop1 and loop12 collectively recognize the target RNA for methylation and are sufficient for the gain of Erm activity. It was further noted that K1 can still recognize 30S ribosomal subunit, but with reduced efficiency (Figure S5A). Thus, it appears that the K1 chimera is a promiscuous version of the selective BsKsgA enzyme. Additionally, the phylogenetic analysis shows that progressive switching of these loops brings KsgA closer to the Erm ancestry (Figure 2D). Hence, subtle changes in loops play a central role in the emergence of resistance by altering targeting.

The in vitro results were corroborated by testing the erythromycin resistance of the chimeras in vivo. Cells transformed with a plasmid containing the competent chimeras were grown at various concentrations of erythromycin and their viability was tested. It was observed that the construct with both loops as well as the head domain-swapped was the best candidate (K3, minimum inhibitory concentration (MIC) ~ 200 μg/mL Figure 4A,B). The loop1 and loop12 swapped chimera (K1) was marginally resistant (MIC ~ 80 μg/mL), whereas K2, the headless variant of K1, was moderately resistant to erythromycin. Neither K2 nor K3 could be expressed in sufficient quantities for in vitro analysis, thus hampering studies of their methylation efficiency. The fact that the loop1 and loop12 switched chimera efficiently methylated mini-RNA substrates in vitro shows that these structural elements suffice for local orientation of the rRNA. In vivo, however, the head domain plays a more critical role in leading the enzyme to the select ribosomal region and serves as a sensor of the global environment.

In conclusion, this work highlights the mechanism through which nature achieves specific targeting in Mtases via either addition or deletion of the flexible loop elements that govern substrate recognition. For instance, the N-terminal loop1 is completely missing in DNA Mtases, as the rigid nature of double-stranded DNA obliterates any need for additional anchoring points. By contrast, larger domains are appended for proteins, in which methylation at a specific residue is more difficult to achieve (Figure S6). Among the rMtases, these loop variations influence the positions they target. In KsgA, these loops are longer because substrate specificity is attained via extensive interaction with both the target site and the surrounding region.[22] On the contrary, in the case of Erms, specificity is achieved owing to the fact that Erms target only precursor ribosomal subunits and the Erm site is inaccessible in mature ribosome. Hence, less complex loop architectures suffice for Erms. Because these loop regions are the divergent elements, specific inhibitors that target only the pathogenic Erms can now be developed. The power of this approach is that this line of design does not target the common SAM binding motif and instead focus on unique RNA selection elements. In the immediate context, inhibitor searches using this strategy can pave the way toward the development of combination therapy aimed at reversing antibiotic resistance.

■ ASSOCIATED CONTENT

Supporting Information

The Supporting Information is available free of charge on the ACS Publications website at DOI: 10.1021/jacs.8b10277.

Materials and Methods (PDF)

DOI: 10.1021/jacs.8b10277
J. Am. Chem. Soc. 2019, 141, 1425−1429

AUTHOR INFORMATION

Corresponding Author

*R. Anand. Telephone: 91-25767165. Fax: 91-25767152. E-mail: ruchi@chem.iitb.ac.in

ORCID

Ruchi Anand: 0000-0002-2045-3758

Notes

The authors declare no competing financial interest.

ACKNOWLEDGMENTS

We thank BM14 and ID29 beamline at European Synchrotron Radiation Facility (ESRF) France, BESSY Synchrotron, Germany and MX2 beamline at Australian Synchrotron for Crystallographic data collection and MALDI-TOF-MS and Scintillation facility at IIT Bombay. We thank Professors Pradeep Kumar P.I., Sandip Kar, Shobhna Kapoor, Arindam Chowdhury, Steven Ealick and Pulak Dutta for critical reading of the paper. This work was funded by SERB/F/4395/2016-17 and 20150237B02RP00614-BRNS.

REFERENCES

(1) Bragginton, E.; Piddock, C.; Laura, J. UK and European Union public and charitable funding from 2008 to 2013 for bacteriology and antibiotic research in the UK: an observational study. *Lancet Infect. Dis.* **2014**, *14*, 857.

(2) Bayer, A. S.; Schneider, T.; Sahl, H.-G. Mechanisms of daptomycin resistance in Staphylococcus aureus: role of the cell membrane and cell wall. *Ann. N. Y. Acad. Sci.* **2013**, *1277*, 139.

(3) Wright, G. D.; Sutherland, A. D. New strategies for combating multidrug-resistant bacteria. *Trends Mol. Med.* **2007**, *13*, 260.

(4) von Wintersdorff, C. J. H.; Penders, J.; van Niekerk, J. M.; Mills, N. D.; Majumder, S.; van Alphen, L. B.; Savelkoul, P. H. M.; Wolffs, P. F. G. Dissemination of Antimicrobial Resistance in Microbial Ecosystems through Horizontal Gene Transfer. *Front. Microbiol.* **2016**, *7*, 173.

(5) Davies, J.; Davies, D. Origins and Evolution of Antibiotic Resistance. *Microbiol Mol. Biol. Rev.* **2010**, *74*, 417.

(6) Blair, J. M. A.; Webber, M. A.; Baylay, A. J.; Ogbolu, D. O.; Piddock, L. J. V. Molecular mechanisms of antibiotic resistance. *Nat. Rev. Microbiol.* **2015**, *13*, 42.

(7) Wright, G. D. The antibiotic resistome: the nexus of chemical and genetic diversity. *Nat. Rev. Microbiol.* **2007**, *5*, 175.

(8) Auerbach, T.; Bashan, A.; Yonath, A. Ribosomal antibiotics: structural basis for resistance, synergism and selectivity. *Trends Biotechnol.* **2004**, *22*, 570.

(9) Almutairi, M. M.; Park, S. R.; Rose, S.; Hansen, D. A.; Vázquez-Laslop, N.; Douthwaite, S.; Sherman, D. H.; Mankin, A. S. Resistance to ketolide antibiotics by coordinated expression of rRNA methyltransferases in a bacterial producer of natural ketolides. *Proc. Natl. Acad. Sci. U. S. A.* **2015**, *112*, 12956.

(10) Vester, B.; Nielsen, A. K.; Hansen, L. H.; Douthwaite, S. ErmE methyltransferase recognition elements in RNA substrates. *J. Mol. Biol.* **1998**, *282*, 255.

(11) Struck, A.-W.; Thompson, M. L.; Wong, L. S.; Micklefield, J. S-Adenosyl-Methionine-Dependent Methyltransferases: Highly Versatile Enzymes in Biocatalysis, Biosynthesis and Other Biotechnological Applications. *ChemBioChem* **2012**, *13*, 2642.

(12) Keating, S.; El-Osta, A. Transcriptional regulation by the Set7 lysine methyltransferase. *Epigenetics* **2013**, *8*, 361.

(13) Daniel, F. I.; Cherubini, K.; Yurgel, L. S.; de Figueiredo, M. A. Z.; Salum, F. G. The role of epigenetic transcription repression and DNA methyltransferases in cancer. *Cancer* **2011**, *117*, 677.

(14) Kozbial, P. Z.; Mushegian, A. R. Natural history of S-adenosylmethionine-binding proteins. *BMC Struct. Biol.* **2005**, *5*, 19.

(15) Bheemanaik, S.; Reddy, Y. V R.; Rao, D. N. Structure, function and mechanism of exocyclic DNA methyltransferases. *Biochem. J.* **2006**, *399*, 177.

(16) Basturea, G. N.; Deutscher, M. P. Substrate specificity and properties of the Escherichia coli 16S rRNA methyltransferase, RsmE. *RNA* **2007**, *13*, 1969.

(17) O'Farrell, H. C.; Scarsdale, J. N.; Rife, J. P. Crystal Structure of KsgA, a Universally Conserved rRNA Adenine Dimethyltransferase in Escherichia coli. *J. Mol. Biol.* **2004**, *339*, 337.

(18) Ochi, K.; Kim, J.-Y.; Tanaka, Y.; Wang, G.; Masuda, K.; Nanamiya, H.; Okamoto, S.; Tokuyama, S.; Adachi, Y.; Kawamura, F. Inactivation of KsgA, a 16S rRNA Methyltransferase, Causes Vigorous Emergence of Mutants with High-Level Kasugamycin Resistance. *Antimicrob. Agents Chemother.* **2009**, *53*, 193.

(19) O'Farrell, H. C.; Musayev, F. N.; Scarsdale, J. N.; Rife, J. P. Binding of Adenosine-Based Ligands to the MjDim1 rRNA Methyltransferase: Implications for Reaction Mechanism and Drug Design. *Biochemistry* **2010**, *49*, 2697.

(20) Demirci, H.; Belardinelli, R.; Seri, E.; Gregory, S. T.; Gualerzi, C.; Dahlberg, A. E.; Jogl, G. Structural rearrangements in the active site of the Thermus thermophilus 16S rRNA methyltransferase KsgA in a binary complex with 5′-methylthio-adenosine. *J. Mol. Biol.* **2009**, *388*, 271.

(21) Goedecke, K.; Pignot, M.; Goody, R. S.; Scheidig, A. J.; Weinhold, E. Structure of the N6-adenine DNA methyltransferase M•TaqI in complex with DNA and a cofactor analog. *Nat. Struct. Biol.* **2001**, *8*, 121.

(22) Boehringer, D.; O'Farrell, H. C.; Rife, J. P.; Ban, N. Structural Insights into Methyltransferase KsgA Function in 30S Ribosomal Subunit Biogenesis. *J. Biol. Chem.* **2012**, *287*, 10453.

(23) Desai, P. M.; Rife, J. P. The adenosine dimethyltransferase KsgA recognizes a specific conformational state of the 30S ribosomal subunit. *Arch. Biochem. Biophys.* **2006**, *449*, 57.

(24) Maravić, G.; Bujnicki, J. M.; Feder, M.; Pongor, S.; Flögel, M. Alanine-scanning mutagenesis of the predicted rRNA-binding domain of ErmC′ redefines the substrate-binding site and suggests a model for protein−RNA interactions. *Nucleic Acids Res.* **2003**, *31*, 4941.

(25) Hansen, L. H.; Lobedanz, S.; Douthwaite, S.; Arar, K.; Wengel, J.; Kirpekar, F.; Vester, B. Minimal Substrate Features for Erm Methyltransferases Defined by Using a Combinatorial Oligonucleotide Library. *ChemBioChem* **2011**, *12*, 610.

(26) Madsen, C. T.; Jakobsen, L.; Buriánková, K.; Doucet-Populaire, F.; Pernodet, J.-L.; Douthwaite, S. Methyltransferase Erm(37) Slips on rRNA to Confer Atypical Resistance in Mycobacterium tuberculosis. *J. Biol. Chem.* **2005**, *280*, 38942.

DOI: 10.1021/jacs.8b10277
J. Am. Chem. Soc. 2019, 141, 1425−1429